

Substrate Binding Causes Movement in the ATP Binding Domain of *Escherichia coli* Adenylate Kinase[†]

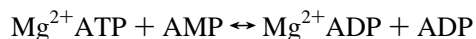
Tim Bilderback,[‡] Tim Fulmer,^{‡,§} William W. Mantulin,^{‡,§} and Michael Glaser^{*,‡}

Department of Biochemistry and the Laboratory for Fluorescence Dynamics, Department of Physics,
University of Illinois, Urbana, Illinois 61801

Received August 7, 1995; Revised Manuscript Received March 11, 1996[®]

ABSTRACT: Crystallographic evidence suggests that there is a large hinged domain motion associated with substrate binding in adenylate kinase. To test this hypothesis, resonance energy transfer measurements of substrate binding were initiated. Adenylate kinase from *Escherichia coli* consists of three domains: the main body of the enzyme with α -helical and β -sheet secondary structure, and domains that close over the AMP and ATP binding sites. Four single tryptophan mutants were constructed to map distances. Two tryptophan mutants were positioned at residues 133 (Y133W) and 137 (F137W), which are in the domain that closes over the ATP binding site. Mutant F86W that is located at the AMP binding site, and mutant S41W that is in the loop that close over AMP, complete the mapping library. Energy transfer was measured between each of these tryptophans and 5-[[2-(acetylamino)ethyl]amino]naphthalene-1-sulfonic acid (AEDANS) covalently bound to the single cysteine residue at position 77, which is located in the main body of adenylate kinase. The distance between the tryptophan of the F137W mutant adenylate kinase and the AEDANS-labeled Cys-77 decreased by 12.1 Å upon the binding of the bisubstrate inhibitor P^1,P^5 -bis(5'-adenosyl) pentaphosphate (AP₅A). There were only small alterations in the tryptophan to Cys-77-AEDANS distances in the Y133W, F86W, and S41W mutants upon the binding of AP₅A, ATP, or AMP, implying that movement of residues 133, 86, and 41 in relation to the Cys-77 residue was minimal. These results suggest that there is significant closure of the ATP binding domain upon the binding of ATP or AP₅A. Unexpectedly, exposure of the enzyme to AMP also introduced a partial closure of the ATP hinged domain.

Adenylate kinases are small (20–26 kDa) monomeric enzymes that catalyze the reaction:



Adenylate kinase functions in the regulation of the concentrations of adenine nucleotides and is the only enzyme that can catalyze the conversion of AMP to ADP (Glaser et al., 1975). Previous studies have suggested that adenylate kinase in skeletal muscle functions as a high energy phosphoryl transfer system regulating ATP production in correspondence with its consumption (Zelevnikar et al., 1995). From comparison of a variety of crystal structures, adenylate kinases are predicted to undergo large domain movements upon binding to substrate (Schulz et al., 1990; Berry et al., 1994), and the study of these movements may aid in understanding kinase function. Recently, the structures of adenylate kinase from several organisms, bound to substrate or in the absence of substrate, have been utilized to make a movie of the proposed motions which occur upon substrate binding (Vonnrhein et al., 1995). The X-ray crystal structure of adenylate kinase from varied species has provided a wealth of structural information about this enzyme; however, understanding its dynamics will require other methods of analysis.

Adenylate kinase crystallographic structures (Müller & Schulz, 1992; Schulz et al., 1990; Berry et al., 1994) and NMR studies (Yan et al., 1990) have revealed separate ATP and AMP binding sites. Predictions, based on the X-ray crystallographic structures, suggest that the AMP binding domain undergoes a movement of 8 Å upon AMP binding and the ATP binding domain moves up to 30 Å upon binding of ATP (Schulz et al., 1990; Gerstein et al., 1993). In part, crystallization forces may drive such large domain motions. The solution structure of the binding sites and the movements, which occur upon substrate binding in the *Escherichia coli* enzyme, are currently unresolved issues.

Fluorescence resonance energy transfer provides a method to map distances in the solution structure of proteins. This method is based on the radiationless transfer of energy through dipole–dipole interactions between an excited state fluorescent donor to an acceptor molecule (Förster, 1948). In turn, the acceptor molecule may or may not be fluorescent.

The use of tryptophan as a fluorescence energy donor requires an acceptor that receives energy at the wavelengths of tryptophan emission. Consequently, the single cysteine residue in *E. coli* adenylate kinase was covalently labeled with IAEDANS. Fluorescence resonance energy transfer was then used to measure distances between the labeled Cys-

[†]This work was supported by the NIH RR03155 and the UIUC.

* Author to whom correspondence should be addressed Department of Biochemistry, University of Illinois, 600 S. Mathews Ave., Urbana, IL 61801. Tel: (217) 333-3960; FAX: (217) 244-5858.

[‡] Department of Biochemistry.

[§] Laboratory of Fluorescence Dynamics.

[®] Abstract published in *Advance ACS Abstracts*, May 1, 1996.

¹ Abbreviations: AEDANS, 5-[[2-(acetylamino)ethyl]amino]naphthalene-1-sulfonic acid; IAEDANS, 5-[[2-[(iodoacetyl)amino]ethyl]amino]naphthalene-1-sulfonic acid; AP₅A, P^1,P^5 -bis(5'-adenosyl) pentaphosphate.

77 residue and unique tryptophan residues introduced by site-directed mutagenesis into the wild-type enzyme, which lacks tryptophan. The distances between Cys-77 and tryptophans introduced into the ATP binding domain at positions 133 and 137 and the AMP binding domain at residues 41 and 86 were measured using energy transfer in the absence of substrate and upon the binding of ATP, AMP, or the bisubstrate inhibitor AP₅A. The distances measured by energy transfer were analyzed to determine the extent of domain motion upon substrate binding. Previously, the 86 and 133 single Trp mutants were used to gain information about the locations of the AMP and ATP binding sites (Liang et al., 1991).

MATERIALS AND METHODS

Sources. IAEDANS was obtained from Sigma Chemical. Gel blue A affinity resin was purchased from Bio-Rad Laboratories. Oligonucleotide-directed mutagenesis kits and [α -³⁵S]dATP were obtained from the Amersham Corp. Oligonucleotide mutagenic primers and a Trp-Pro-Pro-Cys peptide were synthesized by the Biotechnology Center at the University of Illinois.

Site-Directed Mutagenesis. Single Trp residues were introduced into adenylate kinase as previously described (Nakamaya & Eckstein, 1986; Liang et al., 1991). The production of the F86W and Y133W mutants has been described (Liang et al., 1991). The S41W and F137W sequences were verified after subcloning of the mutant adenylate kinase into pUC18 as a *Sma*I–*Hind*III insert containing the adenylate kinase structural gene including its Shine–Delgarno sequence. This plasmid was then expressed in the protease-deficient strain SG21163 (Gottesman, 1990).

Purification of Adenylate Kinase. The mutant adenylate kinases were purified in a manner similar to that previously described (Liang et al., 1991) with the following modifications. The cells were grown at 37 °C and harvested at early stationary phase. After purification using the gel blue A affinity chromatography, the mutant adenylate kinases were dialyzed against four changes of 10 mM Tris, pH 7.4, with 1 mM MgCl₂ (buffer A). The enzyme was applied a second time to the gel blue A resin and washed with buffer A to remove any AP₅A that remained after the elution from the first gel blue A column. The adenylate kinase mutants were eluted with buffer A plus 0.2 M KCl, concentrated using an Amicon stirred cell, and dialyzed against four changes of buffer A.

Labeling with IAEDANS. The F86W, Y133W, S41W, and F137W adenylate kinase mutants and the Trp-(Pro)₃-Cys peptide were labeled with IAEDANS using the method of Gardner and Mathews (1991) with some modifications. After labeling and dialysis, the adenylate kinase mutants were applied to a gel blue A affinity column and washed with buffer A to remove free label. The mutant adenylate kinases were eluted from the column with buffer A plus 0.2 M KCl, concentrated using an Amicon stirred cell, and then dialyzed against four changes of buffer A. The activities of the mutants before and after labeling were monitored using the reverse assay ($\text{Mg}^{2+}\text{ADP} + \text{ADP} \leftrightarrow \text{Mg}^{2+}\text{ATP} + \text{AMP}$) as previously described (Huss & Glaser, 1983). Free label was removed from the Trp-(Pro)₃-Cys peptide by loading the labeled peptide onto a DE 52 ion exchange column that was equilibrated with 10 mM sodium phosphate, pH 7.0, buffer.

The labeled peptide was washed through the column with 10 mM sodium phosphate, pH 7.0, buffer while the free label remained bound to the column. The concentration of the peptide was determined by measurement of the absorbance at 280 nm and using an extinction coefficient for Trp of 5600 M⁻¹ cm⁻¹. The concentration of protein in the labeled adenylate kinase mutants was measured using the method of Lowry et al. (1951). The concentration of AEDANS in the labeled protein or peptide was determined by comparing the fluorescence intensity of AEDANS at 475 nm, when excited at 345 nm, with that of known concentrations of the 1,5-AEDANS 2-mercaptoethanol adduct.

CD Measurements. All CD measurements were performed using a JASCO J-720 spectropolarimeter. The CD spectra were taken using adenylate kinase samples with an absorbance at 222 nm of 1.2 in 10 mM sodium phosphate buffer, pH 7.4. The spectra were obtained at 25 °C using a cell of 0.1 cm path length. Samples were scanned from 250 to 190 nm with a 0.1 nm resolution using a 1.0 nm band width.

Fluorescence Measurements. All fluorescence measurements were performed using a SLM-8000C spectrofluorometer. The band widths for emission and excitation monochromators were 4 nm. Samples of 2 μM labeled or unlabeled adenylate kinase Trp mutants or the Trp-(Pro)₃-Cys peptide in buffer A were excited with light of 295 or 345 nm for energy transfer experiments. Fluorescence emission was monitored at the emission maximum of the Trp donor for measurement of donor-quenching energy transfer using 295 nm excitation, or at the emission maximum of the AEDANS acceptor using both 295 and 345 nm excitation for measurement of acceptor-enhanced emission. The energy transfer measurements were made in the absence and in the presence of either 1 mM AMP, 1 mM ATP, or 20 μM AP₅A. Polarization measurements for AEDANS were performed with excitation at 350 nm and a Corning 3-72 filter in the emission path. Polarization experiments were also carried out in the presence of substrate at the same concentrations as in the energy transfer experiments. Quantum yield measurements for the Trp donor in the adenylate kinase mutants, in the absence and presence of 1 mM AMP, 1 mM ATP, or 20 μM AP₅A, were carried out using excitation at 295 nm and 4 nm band widths. A known concentration of Trp at an approximately equal absorbance was used as a standard assuming a quantum yield of 0.14 (Kirby & Steiner, 1970).

Calculation of Energy Transfer Efficiency from Tryptophan to AEDANS. When a fluorescent molecule is excited, one mode by which it can release this energy is through radiationless transfer to an acceptor molecule. The distance at which energy transfer between a donor and acceptor is 50% efficient, R_0 , (Förster, 1965), was determined using:

$$R_0 = (9.79 \times 10^3)(J\kappa^2 Q_D n^{-4})^{1/6} \text{ \AA} \quad (1)$$

where κ^2 is the angular orientation factor (taken to be $2/3$), Q_D is the quantum yield of the donor in the absence of the acceptor, and n is the refractive index of the medium (taken to be 1.34). The quantum yields of the Trp residues in the various mutants and the peptide control were determined using free tryptophan as a standard (Grossman, 1983). Quantum yields of the Trp adenylate kinase mutants were measured in the presence and absence of 1 mM AMP, 1

mM ATP, and 20 μ M AP₅A. J , the overlap integral between donor emission and acceptor absorbance in eq 1, is given by (Fairclough & Cantor, 1978)

$$J = \frac{\sum F_D(\lambda) \epsilon_A(\lambda) \lambda^4 \Delta\lambda}{\sum F_D(\lambda) \Delta\lambda} \text{ cm}^3 \text{ M}^{-1} \quad (2)$$

where $F_D(\lambda)$ is the fluorescence intensity of the Trp donor at wavelength λ and ϵ_A is the molar extinction coefficient of the acceptor at wavelength λ . To determine J , these values were measured every 5 nm from 300 to 420 nm. The distance between donor and acceptor, R , can be calculated using the equation:

$$R = R_0(E^{-1} - 1)^{1/6} \quad (3)$$

where E is the efficiency of energy transfer between donor and acceptor. E was calculated using the equation:

$$E = 1 - F_{DA}(\lambda)/F_D(\lambda) \quad (4)$$

where F_{DA} is the fluorescence intensity of the donor in the presence of the acceptor and F_D is the fluorescence intensity of the donor alone with both intensities measured at the emission maximum of the donor. E was also calculated using sensitized emission of the acceptor, E_a , which is given by (Tu et al., 1978):

$$E_a = \frac{F_{DA295}^{475} f_{A345} I_{345}}{F_{A345}^{475} f_{D295} I_{295}} \quad (5)$$

where F_{DA295}^{475} is the fluorescence intensity when excited at 295 nm of the donor-acceptor pair, in which the Trp donor was the major absorbing species with fluorescence emission intensity monitored at the AEDANS acceptor's emission maximum of 475 nm, f_A is the fractional absorbance of the acceptor at 345 nm, I_{345} is the intensity of the exciting light at 345 nm, I_{295} is the intensity of exciting light at 295 nm, F_{A345}^{475} is the fluorescence intensity of the AEDANS acceptor at its emission maximum when excited near its absorption maximum, and f_D is the fractional absorbance of the donor Trp at 295 nm.

To eliminate contributions due to direct excitation of the acceptor at 295 nm from the emission measured at 475 nm (F_{A295}^{475}) and to eliminate contributions due to donor emission at 475 nm (F_{D295}^{475}), the following equation was used:

$$F_{DA295}^{475} = F_{\text{total } 295}^{475} - F_{D295}^{475} - F_{A295}^{475} \quad (6)$$

where $F_{\text{total } 295}^{475}$ is the total fluorescence intensity emitted at 475 nm upon excitation of the donor acceptor pair at 295 nm. F_{D295}^{475} was determined directly by exciting an equivalent amount of the donor alone. F_{A295}^{475} was determined by measuring the fluorescence intensity of AEDANS-labeled wild-type adenylate kinase, which has no tryptophan, when excited at 295 nm ($F_{A(\text{wt})295}^{475}$) and also the fluorescence intensity of the same sample when excited at 345 nm ($F_{A(\text{wt})345}^{475}$) and using the values in the following equation:

$$F_{A295}^{475} = F_{A(\text{wt})295}^{475} / F_{A(\text{wt})345}^{475} (F_{DA345}^{475} - F_{D345}^{475}) \quad (7)$$

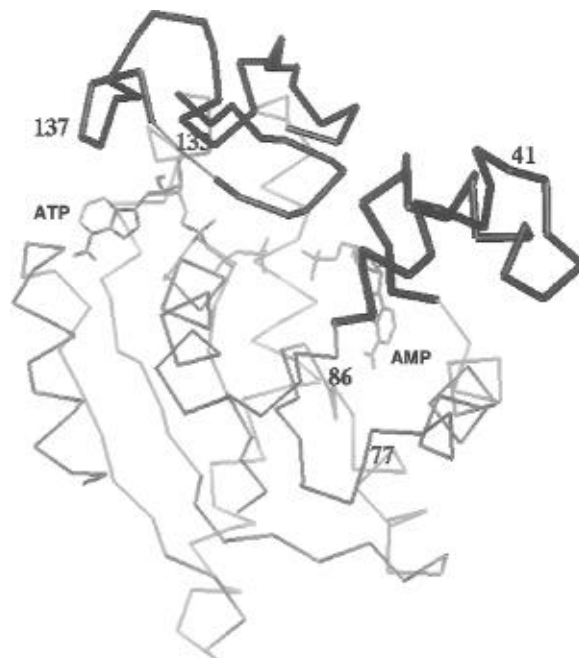


FIGURE 1: The backbone structure of adenylate kinase from *E. coli* based on the coordinates of Berry et al. (1994), with the single Trp mutations indicated at residues 41, 86, 133, and 137. Additionally the position of the AEDANS-labeled Cys-77 residue is shown.

where F_{DA345}^{475} and F_{D345}^{475} are, respectively, the fluorescence intensities of the donor acceptor pair and the donor alone when excited at 345 nm and with emission monitored at the AEDANS emission maxima near 475 nm.

RESULTS

Mutagenesis. Single amino acid residues were replaced by tryptophan at four locations in *E. coli* adenylate kinase (Figure 1). F137W, Y133W, F86W, and S41W were chosen because they are at sites expected to be involved in the binding of substrate (ATP, AMP, and AP₅A). The F137W mutant Trp residue is located in the variable loop that covers bound ATP, the Y133W Trp residue is near the hinge region of the variable loop, the F86W Trp is located in the AMP binding site and is known to alter AMP kinetics, and the S41W Trp residue is in the loop that is predicted to close over AMP (Schulz et al., 1990; Liang et al., 1991).

Labeling. The adenylate kinase single-tryptophan mutants were labeled with IAEDANS under conditions that favor reaction with cysteine (Gardner & Mathews, 1991). The degree of labeling for the single cysteine present in *E. coli* adenylate kinase ranged from approximately 100% in the case of F86W to 16% in the case of F137W, with intermediate levels of labeling obtained for S41W (50%) and Y133W (28%). The variable labeling efficiency between mutants may arise from the relatively shielded location of the cysteine. Additionally, a peptide of Trp-(Pro)₃-Cys was labeled with approximately 100% efficiency. The labeling had relatively small effects on the catalytic activity of adenylate kinase when compared with the unmodified enzyme, and the changes in activity were not dependent upon the degree of labeling (Table 1). The CD spectra showed only slight differences between the mutants and the wild-type enzyme (Figure 2).

Energy Transfer in the Trp-Pro-Pro-Pro-Cys Peptide. As a control, energy transfer from Trp to AEDANS was

Table 1: Specific Activity of Adenylate Kinase before and after Labeling with IAEDANS^a

enzyme	labeling efficiency (%)		specific activity ($\mu\text{mol min}^{-1} \text{mg}^{-1}$)	activity change (%)
wild-type	54	unmodified	261 \pm 28	
		modified	189 \pm 6	-28
S41W	50	unmodified	261 \pm 16	
		modified	248 \pm 32	-5
F86W	100	unmodified	108 \pm 10	
		modified	75 \pm 9	-31
Y133W	28	unmodified	261 \pm 21	
		modified	198 \pm 21	-24
F137W	16	unmodified	330 \pm 31	
		modified	231 \pm 14	-30

^a The specific activity of the enzymes was measured using the reverse assay ($\text{ADP} + \text{Mg}^{2+} + \text{ATP} \leftrightarrow \text{AMP} + \text{Mg}^{2+} + \text{ATP}$).

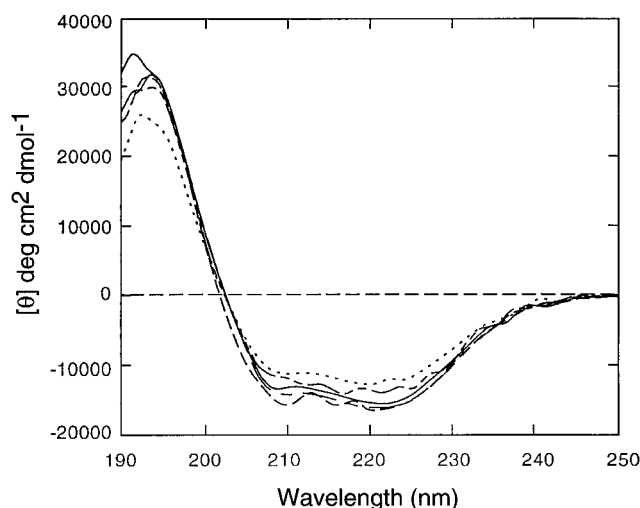


FIGURE 2: The circular dichroism spectra of wild-type (—), S41W (---), F86W (— · —), Y133W (·· · ·), and F137W (— · —) adenylate kinase.

measured in a Trp-(Pro)₃-Cys peptide labeled with AEDANS. The dimensions of polyproline have been measured using X-ray crystallography (Cowen & McGavin, 1955), and the dimensions of this peptide were calculated from this information and molecular modeling to be 23.3 Å. In addition to providing a method of verifying the distances obtained by energy transfer, the peptide was used to examine the effect of having a range of acceptor (AEDANS) to donor (Trp) ratios on energy transfer efficiency. There was good agreement between the donor-to-acceptor distances calculated using acceptor-enhanced emission at all ratios of acceptor used in the adenylate kinase energy transfer experiments (Table 2). Furthermore, the distance of 20.6 ± 0.1 Å calculated using acceptor-enhanced emission agrees very closely with the 23.3 Å distance based on the known dimensions of the rigid polyproline structure and molecular modeling. The donor-quenching data were more dependent on the ratio of donor to acceptor due to error in the measurements, and consequently, the results were more variable than the results obtained using acceptor-enhanced emission (Table 2). Therefore, only the energy transfer efficiency obtained from acceptor-enhanced emission was used in determination of the energy transfer efficiency for the AEDANS-labeled single Trp transfer kinase mutants. Additionally, the effect of substrate addition upon energy

Table 2: Energy Transfer in the Trp-(Pro)₃-Cys AEDANS-Labeled Peptide^a

Trp/AEDANS ^b	E_a (%)	R_a (Å)	E_d (%)	R_d (Å)
0.86	62.6 \pm 1.3	20.7 \pm 0.3	70.1 \pm 1.6	19.5 \pm 0.2
1.71	63.9 \pm 1.0	20.6 \pm 0.1	80.2 \pm 2.3	17.8 \pm 0.4
3.42	64.6 \pm 0.9	20.5 \pm 0.1	92.3 \pm 11.0	14.9 \pm 2.8
6.84	64.7 \pm 2.7	20.5 \pm 0.0	88.7 \pm 24.9	16.0 \pm 4.5

^a R_a is the distance from donor to acceptor calculated using acceptor-enhanced emission, and R_d is the distance calculated using donor-quenching. E_d refers to energy transfer calculated using donor-quenching as in eq 4 with the value normalized to acceptor-donor pairs by multiplying E_d by [donor]/[acceptor] ([Trp]/[AEDANS]). ^b The Trp/AEDANS ratio was varied by addition of unlabeled peptide to labeled peptide maintaining a total peptide concentration of 2 mM.

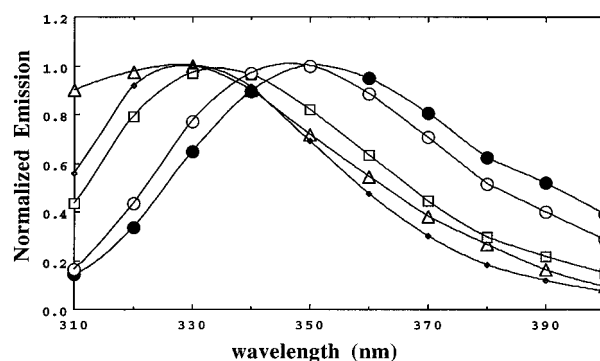


FIGURE 3: The normalized emission spectra of the S41W (●), F86W (●), Y133W (□), F137W (○), and AEDANS normalized absorption spectrum (Δ).

transfer in the peptide was examined. There was no significant change in E_a upon the addition of 1 mM AMP, 1 mM ATP, or 20 μM AP_5A , demonstrating that addition of these compounds did not affect the measurements.

Energy Transfer in Adenylate Kinase. Excitation at 295 nm of the tryptophan residues in the adenylate kinase mutants resulted in emission maxima ranging from 326 nm for F86W to 352 nm for S41W, with Y133W and F137W having intermediate values for the emission maximum (Figure 3). These mutants exhibited insignificant shifts (<3 nm) in tryptophan emission maxima upon labeling with IAEDANS or upon the addition of substrate. The differences in emission maxima due to the different environments of the Trp mutants and the changes in the overlap with the absorption of AEDANS (Figure 3) were considered in the calculation of the overlap integral (J). Quenching of tryptophan emission upon labeling or binding of substrate was also considered in determining the value for J and in the quantum yield (Table 3). When the single Trp containing adenylate kinases were labeled with IAEDANS and excited at 295 nm, the emission of Trp was reduced in comparison to the unlabeled protein. Concurrently, there was fluorescence emission at approximately 475 nm, which corresponds to AEDANS fluorescence.

The efficiency of energy transfer varied significantly between the mutant adenylate kinases (Table 3). The F86W mutant had the highest efficiency in the absence of substrate, followed by Y133W, S41W, and F137W. These efficiencies were used to calculate the distance from the AEDANS-labeled Cys-77 to each single Trp residue using eqs 1–6 (Table 3).

The energy transfer efficiencies for the F137W mutant increased from $5.6 \pm 0.8\%$ in the absence of substrate to

Table 3: Energy Transfer Measurements for AEDANS-Labeled Adenylate Kinase

mutant	J^a	% energy transfer ^b	R_0 (Å) ^c	R (Å)	ΔR (Å)
S41W	6.13×10^{-15}	10.0 ± 0.7	24.0	34.6 ± 0.4	
+AMP	6.20×10^{-15}	10.3 ± 1.7	23.0	33.0 ± 1.0	$+1.6 \pm 1.1$
+ATP	6.16×10^{-15}	9.2 ± 1.0	23.8	34.9 ± 0.7	-0.3 ± 0.8
+AP ₅ A	6.13×10^{-15}	10.1 ± 2.4	22.7	32.8 ± 1.3	$+1.8 \pm 1.4$
F86W	6.34×10^{-15}	44.5 ± 1.7	22.8	23.7 ± 0.2	
+AMP	6.30×10^{-15}	35.2 ± 1.9	22.3	24.7 ± 0.4	-1.0 ± 0.5
+ATP	6.14×10^{-15}	38.1 ± 4.3	22.2	24.1 ± 0.7	-0.4 ± 0.7
+AP ₅ A	6.62×10^{-15}	32.6 ± 1.2	20.6	23.3 ± 0.2	$+0.4 \pm 0.2$
Y133W	6.67×10^{-15}	17.8 ± 0.3	22.8	29.5 ± 0.1	
+AMP	6.31×10^{-15}	19.4 ± 2.5	22.1	28.1 ± 0.8	$+1.4 \pm 0.8$
+ATP	6.16×10^{-15}	18.4 ± 1.0	21.7	27.8 ± 0.3	$+1.7 \pm 0.3$
+AP ₅ A	6.62×10^{-15}	17.7 ± 1.6	21.5	27.8 ± 0.6	$+1.7 \pm 0.6$
F137W	6.37×10^{-15}	5.6 ± 0.8	21.0	33.7 ± 0.8	
+AMP	6.32×10^{-15}	19.1 ± 3.4	20.4	26.0 ± 0.9	$+7.7 \pm 1.2$
+ATP	6.09×10^{-15}	17.4 ± 0.2	19.3	25.0 ± 0.1	$+8.7 \pm 0.8$
+AP ₅ A	6.12×10^{-15}	25.6 ± 6.8	18.0	21.6 ± 1.3	$+12.1 \pm 1.5$

^a The overlap integral (J) was calculated using eq 2, and differences in J are due to small changes in the Trp emission spectra upon binding of substrate or due to the different environments of Trp in different mutants. ^b Calculated using acceptor-enhanced emission efficiency (eq 5). ^c Calculated using eq 1, with changes in R_0 resulting from alterations in J and quantum yield changes in Trp emission upon substrate binding.

$25.6 \pm 6.8\%$ when $20 \mu\text{M}$ AP₅A was added. This efficiency change corresponded to a decrease in distance between donor and acceptor of 12.1 \AA . Addition of 1 mM AMP to F137W increased energy transfer efficiency from $5.6 \pm 0.8\%$ to $19.1 \pm 3.4\%$, and the corresponding distance between donor and acceptor decreased by 7.7 \AA . In the presence of 1 mM ATP, the energy transfer efficiency for F137W increased from $5.6 \pm 0.8\%$ to $17.4 \pm 0.2\%$, indicating an 8.7 \AA decrease in the distance from the donor to acceptor.

The changes in energy transfer efficiency for S41W, Y133W, and F86W upon substrate binding were not significant, suggesting that these residues did not move greatly in relation to Cys-77 upon substrate binding. In the S41W mutant, the Cys-77 AEDANS to Trp distance decreased 1.6 \AA upon AMP binding and 1.8 \AA upon AP₅A binding, but moved only 0.3 \AA upon ATP binding. The Y133W mutant also showed modest movements upon substrate binding, with the Cys-77 AEDANS to Trp distance decreasing by 1.4 \AA upon AMP binding, 1.7 \AA upon ATP binding, and 1.7 \AA upon AP₅A binding. In the F86W mutant, the changes were all 1.0 \AA or less. The levels of substrates used in these experiments saturated the enzyme binding sites.

An important consideration in calculating the distances between donor and acceptor is the angular orientation factor κ^2 . The κ^2 term reflects the ability of the donor and acceptor to randomize their orientations by rotational diffusion. The values for this factor can range from 0 to 4, but a value of κ^2 equal to $2/3$ can be assumed if the donor and acceptor, are free to rotate. In order to examine the rotational freedom of the acceptor, steady-state polarization values were determined for AEDANS in each mutant adenylate kinase in the presence or absence of the substrates used for energy transfer efficiency (Table 4). In general, the polarization values were similar for all the mutants and the wild-type enzyme. When a substrate was added, either AP₅A, ATP, or AMP, the values were slightly lower, reflecting a small change in the AEDANS environment. In all cases, the polarization value indicated considerable motional freedom, and this indicates

Table 4: AEDANS Polarization for Labeled Adenylate Kinase

enzyme	polarization			
	no substrate	$20 \mu\text{M}$ AP ₅ A	1 mM ATP	1 mM AMP
native	0.110	0.096	0.100	0.090
S41W	0.127	0.099	0.100	0.116
F86W	0.133	0.108	0.084	0.112
Y133W	0.112	0.116	0.106	0.102
F137W	0.125	0.097	0.106	0.106

that the error in the calculated energy transfer distance is less than 10% when using the assumption that κ^2 equals $2/3$ (Haas et al., 1978). The polarization values for Trp residues were generally low (<0.2), and they reflected the differences in their environment (Fulmer et al., 1995).

DISCUSSION

The methods of fluorescence donor-quenching energy transfer and sensitized acceptor-enhanced energy transfer were compared for a peptide of known dimensions. The method of measuring energy transfer efficiency using sensitized acceptor-enhanced energy transfer proved to be superior to donor-quenching in terms of consistency of distances calculated over a range of acceptor to donor ratios. At low labeling efficiencies, it is necessary to correct for this low efficiency so that only a donor which also has an acceptor attached to the peptide is considered when using donor-quenching to calculate the energy transfer efficiency. An additional source of error in the donor-quenching measurements is the preparation of duplicate labeled and unlabeled sample pairs where differences in the protein concentration between two samples can result in large errors in the energy transfer efficiency. Neither of these sources of error is relevant when calculating acceptor-enhanced energy transfer efficiency, which involves only peptides with donor acceptor pairs. Here each acceptor is bound to a donor, and only acceptor emission is being monitored. Also, the same sample is used to calculate both fluorescence intensity terms in the equation for acceptor-enhanced energy transfer efficiency (eq 5), eliminating the need to make duplicate samples. Additionally, the distances between donor and acceptor obtained by energy transfer using acceptor-enhanced measurements were nearly identical to those predicted from the molecular dimensions of the rigid polypeptide peptides. In proteins there is also the additional concern that there could be a difference in the environment of the donor between the labeled and unlabeled protein, and this could cause changes in the quantum yield of the donor affecting the apparent donor-quenching efficiency. For these reasons, acceptor-enhanced emission was used to determine distances from Trp to AEDANS in the adenylate kinase single Trp mutants.

In order to monitor the movement of various regions of adenylate kinase upon substrate binding, Trp residues were introduced into the AMP and ATP binding domains. The single Cys-77 residue located in the main body of adenylate kinase was labeled with AEDANS, making possible fluorescence resonance energy transfer from the single Trp residues to the AEDANS. The efficiency of energy transfer was then used to determine the distance from the AEDANS-labeled Cys-77 residue to the Trp residue in the presence or absence of AMP, ATP, or the bisubstrate inhibitor AP₅A.

The binding of substrates to the single Trp adenylate kinase mutants resulted in significant changes in the distance between the AEDANS-labeled Cys-77 residue and the 137 Trp residue in the mobile ATP binding domain. The 137W residue, located in the variable loop that covers the bound ATP, moved 12.1 Å closer to the AEDANS acceptor upon AP₅A binding, 8.7 Å closer upon ATP binding, and 7.7 Å closer when AMP alone was bound. The large movement seen upon AP₅A binding agrees with the observation that AP₅A associates very tightly with adenylate kinase based upon dissociation constants for this bisubstrate analog (Liang et al., 1991). The observation that ATP causes the ATP binding domain to move was expected, but the finding that AMP causes a movement of similar magnitude in the ATP binding domain was somewhat unexpected in view of X-ray crystallographic comparisons of adenylate kinases. In these studies the core structures of the adenylate kinases from porcine muscle without ligand, bovine heart mitochondria bound to AMP, and *E. coli* bound to AP₅A were superimposed, and this information was used to predict the movement of the AMP and ATP binding domains during catalysis (Schulz et al., 1990). The comparison of these structures led to the conclusion that the AMP binding domain alone closes in response to the binding of AMP. Additionally, these comparisons led to the conclusion that there is movement of both the AMP and ATP binding domains upon the binding of ATP when AMP is already bound. The crystallographic comparisons could be misleading if the enzymes from these different sources were not comparable in the extent and degree of movement. There are numerous differences between these adenylate kinases including the 30 amino acid addition to the ATP binding loop in bacterial adenylate kinases, in comparison with the mammalian cytosolic form. The *E. coli* enzyme shows strong uncompetitive substrate inhibition by AMP while the rabbit muscle adenylate kinase shows only very weak substrate inhibition. Also, the beef heart mitochondrial form preferentially uses GTP in the phosphorylation of AMP as opposed to the other adenylate kinases. In view of such variations between adenylate kinases, it is possible that the structural comparisons may not be entirely valid.

One explanation for the movement in the ATP binding domain upon addition of AMP is that AMP binds to the ATP site and this induces closure. Kinetic data indicate that AMP is an uncompetitive inhibitor toward ATP in adenylate kinase from *E. coli*, which argues against strong binding of AMP to the ATP site (Liang et al., 1991; Huss et al., 1989). If AMP binds to the ATP binding site, it would be surprising that this would cause a change in distance between Cys-77 and Trp-137 nearly equal to that resulting from ATP addition, since the β phosphate of ATP forms five hydrogen bonds with adenylate kinase main chain atoms and makes contacts with the side chains of Arg-123 and Lys-13. Additionally, the γ phosphate forms hydrogen bonds to the side chains of Lys-13, Arg-123, and Arg-156 (Müller & Schulz, 1992). This indicates that 10 of 15 hydrogen bonds stabilizing ATP binding would not be present for AMP binding. The loss of this much stabilization energy, along with the loss of contacts with Arg-123 and Arg-156 in the ATP binding loop, would be expected to significantly reduce the ability of AMP to bind to the ATP site and cause the same conformational change as ATP.

An alternative explanation is that the binding of AMP to the AMP binding site causes movement in the ATP binding domain. One study which supports the binding of AMP preferably to the AMP site in the absence of ATP showed that site-directed affinity probes could be directed to the AMP or ATP binding sites by protection of the second site with saturating levels of substrate (Pranab et al., 1992). It has also been observed that binding of AMP can cause enhancement of fluorescence for probes bound to the ATP site, supporting the model where AMP causes conformational changes in the ATP site upon binding to the AMP site (Chaun et al., 1989). Kinetic studies of adenylate kinase from various sources reveal a rapid equilibrium random sequential mechanism for adenylate kinase (Rhoads & Lowenstein, 1968; Su & Russel, 1968; Markland & Wadkins, 1966; Font & Gautheron, 1980; Huss et al., 1989). In enzymes having this mechanism, both substrates bind randomly to the enzyme. The binding of one substrate changes the dissociation constant for the second substrate and *vice versa*. It has been proposed that the closure of the ATP binding domain upon AMP binding would explain the uncompetitive inhibition observed for AMP at concentrations above 0.2 mM for *E. coli* adenylate kinase, since AMP could bind prior to release of ADP resulting in the formation of an abortive complex (Liang et al., 1991). This is a plausible model that would explain the significant inhibition of adenylate kinase at AMP concentrations greater than 0.2 mM in the presence of saturating ATP.

The S41W mutant Trp residue located in the AMP binding domain did not move significantly in relation to Cys-77 upon AMP or ATP binding. The AMP binding domain is not predicted to undergo as dramatic a movement as the ATP binding domain (Schulz et al., 1990; Berry et al., 1994), and even though no change in distance between the energy transfer donor and acceptor was observed, this does not preclude movement that would not change this distance. In the case of the Y133W mutant there was also no significant movement between Trp and the AEDANS-labeled Cys-77 residue. Comparison of the X-ray crystal structures of adenylate kinases where substrate is bound and those formed in the absence of substrate suggests that both the F137W and the Y133W residue would move upon substrate binding (Schulz et al., 1990). However, 133W is positioned near the hinge region of the ATP binding domain, and the movement of this residue may be small. The F86W mutant whose Trp is located at the AMP binding site also underwent little movement upon the binding of substrate. This is consistent with predictions based on the X-ray structures of adenylate kinases from several sources in the presence and absence of substrate (Schulz et al., 1990).

The distances between the donor and acceptor in adenylate kinase calculated using energy transfer were greater than those predicted by the crystal structure except in the case of the F137W mutant. The crystal structure for *E. coli* adenylate kinase bound to AP₅A (Müller & Schulz, 1992) predicted an approximately 10 Å shorter distance from 41W and 86W to Cys-77 than that calculated using energy transfer in the presence of AP₅A. The same crystal structure predicted an approximately 10 Å longer distance from 137W to Cys-77 than that determined using energy transfer. However, the crystal structure distance predicted for the 133W residue to Cys-77 was within 3 Å of the distance calculated using energy transfer efficiency. The addition of

the Trp residue and the AEDANS molecule could change the distance between Cys-77 and the various Trp residues. Depending on the orientation of the AEDANS, this could either increase or decrease the distance in comparison to the crystal structure distances. It should also be noted that the energy transfer distances are the average distances between donor and acceptor in a solution structure, and this distance may not be the same as that seen in the X-ray crystal structure.

In conclusion, energy transfer was used to observe changes in distance between the Cys-77 residue and the AMP and ATP binding domains upon the binding of substrates. A large change in the ATP binding domain occurred upon either ATP or AMP binding, and this is consistent with the mechanism of adenylate kinase involving a series of interactions between binding domains.

ACKNOWLEDGMENT

We thank Dr. Susan Gottesman for generously providing us with the protease-deficient strain SG21163. We wish to express our appreciation to John Harvey for his generous help in preparation of the figures. We also thank Dr. Ruth Welti for helpful advice during the preparation of the manuscript.

REFERENCES

- Berry, M. B., Meador, B., Bilderback, T., Liang, P., Glaser, M., & Phillips, G. N., Jr. (1994) *Proteins* 19, 183–198.
 Chaun, H., Lin, J., & Wang, J. H. (1989) *J. Biol. Chem.* 264, 7981–7988.
 Cowan, P. M., & McGavin, S. (1955) *Nature* 176, 501–503.
 Dale, R. E., & Eisinger, J. (1974) *Biopolymers* 13, 1573–1605.
 Fairclough, R. H., & Cantor, C. R. (1978) *Methods Enzymol.* 48, 347–349.
 Font, B., & Gautheron, D. C. (1980) *Biochim. Biophys. Acta* 611, 299–308.
 Förster, T. (1948) *Ann. Phys. (Leipzig)* 2, 55–75.
 Förster, T. (1965) in *Modern Quantum Chemistry* (Sinanoglu, O., Ed.) pp 93–137, Academic Press, New York, NY.

- Fulmer, T., Bilderback, T., Glaser, M., & Mantulin, W. W. (1995) In preparation.
 Gardner, J. A., & Mathews, K. S. (1991) *Biochemistry* 30, 2707–2712.
 Gerstein, M., Schulz, G., & Chothia, C. (1993) *J. Mol. Biol.* 229, 494–501.
 Glaser, M., Nulty, W., & Vagelos, P. R. (1975) *J. Bacteriol.* 123, 128–136.
 Gottesman, S. (1990) *Methods Enzymol.* 185, 119–129.
 Grossman, S. H. (1983) *Biochemistry* 22, 5369–5375.
 Haas, E., Katchalski-Katzir, E., & Steinberg, I. Z. (1978) *Biochemistry* 17, 5064–5070.
 Huss, R. J., & Glaser, M. (1983) *J. Biol. Chem.* 258, 13370–13376.
 Huss, R. J., Ruggiero, V. U., & Glaser, M. (1989) Unpublished data.
 Kirby, E. P., & Steiner, R. F. (1970) *J. Phys. Chem.* 74, 4480–4490.
 Liang, P., Phillips, G. N., Jr., & Glaser, M. (1991) *Proteins* 9, 28–36.
 Lowry, O. H., Rosebrough, N. J., Farr, A. L., & Randall, R. J. (1951) *J. Biol. Chem.* 193, 265–275.
 Markland, F. S., & Wadkins, C. L. (1966) *J. Biol. Chem.* 241, 4136–4145.
 Müller, C. W., & Schulz, G. E. (1992) *J. Mol. Biol.* 224, 159–177.
 Nakamaye, K., & Eckstein, F. (1986) *Nucleic Acids Res.* 14, 9679–9698.
 Pranab, P. K., Zhenping, M., & Coleman, P. S. (1992) *J. Biol. Chem.* 267, 25003–25009.
 Reinstein, J., Brune, M., & Wittinghofer, A. (1988) *Biochemistry* 27, 4712–4720.
 Rhoads, D. G., & Lowenstein, J. M. (1968) *J. Biol. Chem.* 243, 3963–3972.
 Schulz, G. E., Müller, C. W., & Diedrichs, K. (1990) *J. Mol. Biol.* 213, 627–630.
 Su, S., & Russel, P. J. (1968) *J. Biol. Chem.* 243, 3826–3833.
 Vonnrhein, C., Schlauderer, G. J., & Schulz, G. E. (1995) *Structure* 3, 483–490.
 Yan, H., Shi, Z., & Tsai, M. (1990) *Biochemistry* 29, 6385–6392.
 Zeleznikar, R. J., Dzeja, P. P., & Goldberg, N. D. (1995) *J. Biol. Chem.* 270, 7311–7319.

BI951833I